J. Electrochem. Sci. Eng. **12(4)** (2022) 787-797; http://dx.doi.org/10.5599/jese.1381

Open Access : : ISSN 1847-9286
www.jESE-online.orghttp://www.jese-online.org/

Original scientific paper

Char of *Tagetes erecta* (African marigold) flower as a potential electrode material for supercapacitors

Venkata Naga Kanaka Suresh Kumar Nersu[1,✉], Bhujanga Rao Annepu[1], Subhakaran Singh Rajaputra[2] and Satya Srinivasa Babu Patcha[3]

[1]*Department of Instrument Technology, Andhra University College of Engineering (A), Visakhapatnam, Andhra Pradesh 530003, India*

[2]*Centre for Advanced Energy Studies, Koneru Lakshmaiah Education Foundation, Vaddeswaram, AP, India*

[3]*Center for Flexible Electronics, Department of Electronics and Communication Engineering, Koneru Lakshmaiah Education Foundation, Vaddeswaram, AP, India*

Corresponding author: ✉sureshk834@gmail.com

Received: May 16, 2022; Accepted: July 9, 2022; Published: July 25, 2022

Abstract

A char of Tagetes erecta *flowers (TFC) was derived through simple thermal decomposition of* Tagetes erecta *flowers (TF). Physico-chemical properties of as-prepared TFC were evaluated using XRD, FESEM, FTIR, TGA, N_2 adsorption-desorption isotherm analysis and water contact angle measurements. The practicality and applicability of TFC as promising electrode material in supercapacitors (SCs) were evaluated in full-cell configuration by performing electrochemical characterizations like CV, GCD and EIS on a lab-scale TFC-based symmetric SC. TFC exhibited a remarkable specific capacitance of 118.4 F g^{-1} at a constant current density of 0.2 A g^{-1} and a specific energy of 4.1 Wh kg^{-1} at specific power of 0.1 kW kg^{-1}. TFC showed excellent cyclic stability by retaining 92 % of its initial capacitance even after 6000 GCD cycles at 2 A g^{-1}. The superior capacitive behaviour and cyclic stability of TFC could be attributed to its good wettability towards water. This excellent supercapacitive performance of TFC establishes it as a potential floral waste-derived carbon-based electrode material for SCs.*

Keywords

Biochar; flowers waste; gel polymer electrolyte; electric double-layer capacitor (EDLC); carbon cloth; hydrophilicity

Introduction

In India, nearly 300,000 hectares are under floriculture producing nearly 3 million tons of flowers annually (as per National Horticulture Board of India statistics of 2018-2019). Flowers like rose, marigold (*Tagetes erecta*), jasmine, hibiscus, *etc.*, are most commonly used in the preparation of garlands, decoration of religious sites and statues during festivals, as well as offerings during

weddings and other ceremonies [1]. After serving their purpose, these flowers are left unused and are usually dumped in soil or disposed into water bodies [2]. Daily, around 40 % of flowers produced in India are left unsold, generating a huge amount of floral waste [3].

Disposing floral waste in open landfills would attract microorganisms that degrade it, thereby releasing harmful gases like methane, carbon dioxide and ammonia, developing a foul smell, and promoting greenhouse emissions [4]. In India, floral waste is dumped in rivers and other water bodies resulting in serious water pollution [5,6]. Disposal of flower waste is a major concern to the environment and there is a need for novel methods to convert floral waste into value-added products [3]. Currently, flower waste is being utilized for the preparation of compost, eco-friendly incense sticks, soaps, as well as conditioners in lawn dressing [7].

Eco-friendly energy storage devices are of utmost importance in the current scenario as alternatives to storing energy harvested from renewable energy sources [8]. Electric double-layer capacitors (EDLCs) are a type of supercapacitors (SCs) that store charge in the form of an electric double layer (EDL) at the electrode-electrolyte juncture and are familiar for their superior charge-discharge capability and long cyclic life [9]. Carbon-based materials are often used as electrode materials in EDLCs and commercially available EDLCs use activated carbon as electrode material [10]. Recently, the development of low-cost and eco-friendly electrode materials such as biological waste-derived carbon-based materials has gained a lot of attention from scientific communities worldwide [11].

Carbons obtained from bamboo [12], sunflower stems [13], lotus stems [14], rice straw [15], wheat straw [16], corn stalks [17], cotton stalks [18], and sugar cane bagasse [19] were already tested as electrode materials in SCs. Wood sawdust [20] and wood [21] were also used to derive carbons and tested as electrode materials in SCs. Carbons obtained from hemp fibers [22], bamboo fibers [23], jute fibers [24], lotus leaves [25], eucalyptus leaves [26], *ficus religiosa* leaves [27] and pine leaves [28] were tested for their potential as electrode materials in SCs. Rice husk [11] and shells of coconuts [29], oil palm kernel [30], and macadamia nuts [31] were used as precursors to derive carbon-based electrode materials for SCs. Biological waste of animal origin like scales of fish [32], hair of human beings [33], shells of shrimps [34] and chicken eggs [35] and chicken feathers [36] were used to derive carbon-based electrode materials for SCs. In the past, flowers like cherry blossom [37], rose [38] and catkins of willow [39-42] were used to derive carbon-based materials and applied as electrode materials in SCs.

Flowers of *Tagetes erecta* (TF), also known as African or Mexican marigold, are commonly used for decoration, extraction of carotenoids and essential oils, adding colour to food items and medicinal purposes [43]. In India, around 3910 hectares of area is under marigold cultivation with an average yield of 22.4 tons per hectare [44], and producing nearly 87,000 tons of TF per year. Disposal of the resulting floral waste requires strategies like the production of bioethanol from TF waste, *etc.* [2]. Gupta *et al*. [45] reported the synthesis of graphene quantum dots from TF and tested its potential as electrode material in SCs in a three-electrode configuration.

In the present work, char of *Tagetes erecta* flower (TFC) was obtained by facile thermal decomposition of TF excluding activation steps making the procedure eco-friendly. Physico-chemical properties of TFC were investigated. A TFC-based SC (full-cell) was constructed using TFC, hydrothermally reduced carbon cloth (CCHy), graphene incorporated sulfonated polyvinyl alcohol (SPVA-HRG-0.5) hydrogel, and Whatman® filter paper as electrode material, current collector, electrolyte and porous separator, respectively. Supercapacitive performance of the constructed cell was investigated using electrochemical techniques like cyclic voltammetry (CV), galvanostatic charge-discharge (GCD) and electrochemical impedance spectroscopy (EIS).

Experimental

Materials

TF waste was collected from nearby temples of Andhra Pradesh, India. Carbon cloth was procured from Avcarb, USA. Multiwalled carbon nanotubes (MWCNTs) were procured from Ad Nano technologies, India. Sulfuric acid (H_2SO_4) (98 %), hydrogen peroxide (H_2O_2) (30 % w/v), graphite (<20 μm), sodium nitrate ($NaNO_3$), polyvinylidine difluoride (PVDF) (MW ~320,000), ethanol (99.9 %), sodium hydroxide (NaOH), polyvinyl alcohol (PVA) (MW ~1,25,000), nitric acid (HNO_3), isopropanol (IPA), hydrochloric acid (HCl) (35-38 %), N-methyl-2-pyrrolidone (NMP) and potassium permanganate ($KMnO_4$) were used as received. Whatman® qualitative filter paper was procured locally and used as a separator during the fabrication of TFC-based SC. Deionized (DI) water was utilized throughout the synthesis.

Preparation of TFC

Collected TF were washed with DI water and dried at room temperature (RT). Trimmed petals of TF were placed in a crucible and covered with aluminum foil in which tiny holes were made for the elimination of volatile compounds while thermal decomposition. TF petals were heated for 3 h at 350 °C to obtain TFC (Figure 1).

Figure 1. *Preparation of TFC through thermal decomposition of TF*

Preparation of CCHy

CCHy was prepared from commercially acquired carbon cloth following the synthesis procedure reported elsewhere [46]. Carbon cloth was dropped into a 2:1 mixture (30 mL) of H_2SO_4 and HNO_3, and $KMnO_4$ (3 g) was added to the mixture while agitating at RT. Later, DI water (100 mL) was added to the mixture and stirred for 3 h continuously, followed by the addition of 30 % H_2O_2 (5-10 mL), leading to the formation of a transparent solution. The obtained oxidized carbon cloth was cleaned many times with DI water and later transferred into a DI water-filled polytetrafluoroethylene (PTFE) lined autoclave and heated for 14 h at 180 °C to obtain CCHy. Collected CCHy was dried and later used as a current collector in the fabrication of TFC-based SC.

Preparation of NGPE

Hydrothermally reduced graphene oxide (HRG) was synthesized following the procedure reported elsewhere [47]. Graphite (2 g) was dispersed into a mixture of H_2SO_4 (98 mL) and $NaNO_3$ (2 g) and agitated for 4 h continuously by preserving the suspension temperature under 5 °C using an ice bath. To this suspension, $KMnO_4$ (12 g) was slowly added and stirred for 2 days continuously at RT. The temperature of the suspension was further decreased to <5 °C using an ice bath and then DI water (184 mL) was added to the suspension and stirred for another 2 h. Finally, 30 % H_2O_2 was slowly added to the suspension while stirring until the suspension color changed yellow, signifying graphene oxide (GO) formation. The yellow-coloured suspension was kept a side to allow sedimentation of GO. Later, the supernatant solution was decanted to obtain GO precipitate, which was washed and centrifuged multiple times using 1 M HCl and DI water until color of GO precipitate turned black. Finally, the GO precipitate was cleansed using ethanol and later centrifuged and vacuum dried for 12 h at 70 °C to obtain GO films, which were further powdered to obtain GO. Later, GO (0.2 g) was dispersed into DI water (200 mL) and transferred into a PTFE-lined autoclave while maintaining pH at 11 using NaOH pellets. The autoclave was heated at 180 °C for 14 h and the collected HRG was vacuum dried at 60 °C for 12 h to acquire HRG.

NGPE was prepared by incorporating HRG into sulfonated PVA hydrogel to obtain HRG incorporated sulfonated PVA hydrogel (SPVA-HRG-0.5) following the procedure reported elsewhere [48]. To DI water (4 mL), H_2SO_4 (270 μL) was added and heated up to 80 °C followed by the addition of PVA (0.5 g) and stirred until a clear sulfonated PVA (SPVA) hydrogel was obtained. Finely powdered HRG (25 mg) was dispersed in IPA (10 mL) and this dispersion was slowly added into SPVA hydrogel while stirring at 80 °C for 0.5 h to obtain SPVA-HRG-0.5, where 0.5 represents the wt.% of HRG in SPVA hydrogel. The as-prepared NGPE was used as an electrolyte in the fabrication of TFC-based SC.

Characterization studies

The structural properties of TF and TFC were analyzed utilizing X-ray diffraction (XRD) technique (Rigaku miniflex 600). The functional groups present in TF and TFC were determined using Fourier-transform infrared (FTIR) spectroscopy (Cary 630). Field emission scanning electron microscopy (FESEM) (FEI-Quanta FEG 200F) was used to investigate the surface morphology of TFC. The surface area and porosity profile of TFC was evaluated using a surface area and porosity analyser (Quantachrome Nova 2200e). Thermogravimetric analysis (TGA) (Simultaneous thermal analyser - STA 7200, Hitachi HTG) of TFC was carried out under N_2 atmosphere up to 800 °C at a heating rate of 20 °C min^{-1}. A pellet of TFC (diameter = 1.2 cm) was prepared to perform water contact angle measurement (Kyowa DM-501) through the sessile drop technique. A lab-scale TFC-based symmetric SC was fabricated by sandwiching TFC-coated CCHy on either side of a SPVA-HRG-0.5 electrolyte soaked Whatman® filter paper. The supercapacitive behaviour of TFC-based symmetric SC (full-cell) was tested using an electrochemical workstation (PARSTAT PMC 2000A) by performing CV, GCD and EIS techniques. TFC, MWCNTs and PVDF were dispersed in NMP in the ratio of 80:10:10 to obtain an electrode ink, which was later coated over two CCHy (area of each CCHy = 0.8 cm^2) and heated at 120 °C for 15 min under vacuum, resulting in TFC coated CCHy (TFC-CCHy) with a TFC loading of 1 mg cm^{-2}. A full cell was fabricated by sandwiching a pair of TFC-CCHy on either side of a SPVA-HRG-0.5 gel polymer electrolyte soaked Whatman® filter paper.

Results and discussion

Physico-chemical characterizations

Figure 2 (a) illustrates the diffraction patterns of TF and TFC showing characteristic broad peaks, indicating the presence of amorphous carbon and the peaks in TFC are less sharp compared to TF, indicating an increase in its amorphous nature after thermal decomposition [49,50].

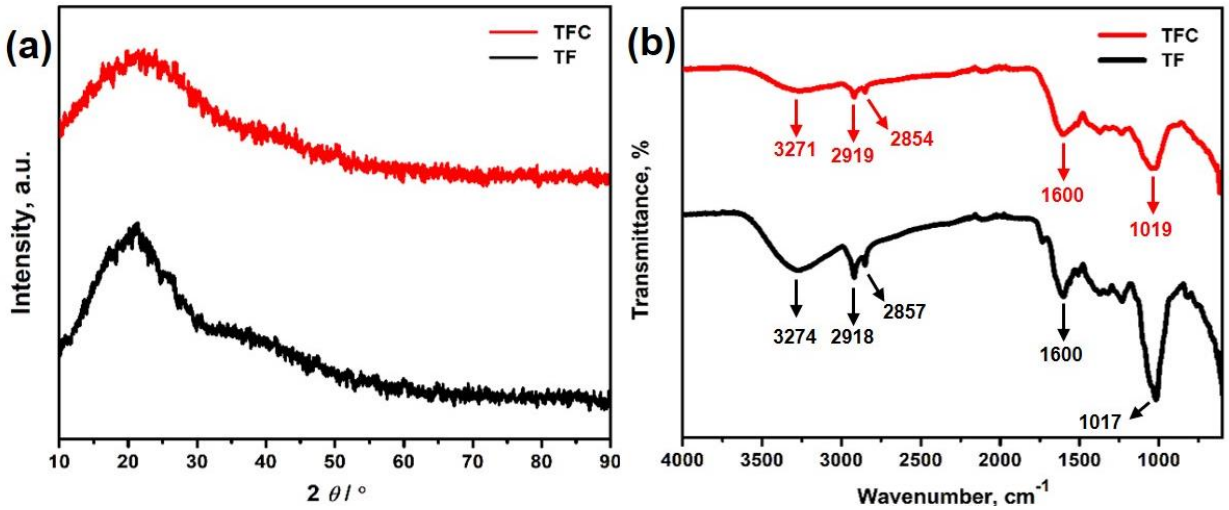

Figure 2. *(a) X-ray diffractograms and (b) FTIR spectra of TF and TFC, respectively*

Figure 2(b) illustrates the FTIR spectra of TF and TFC. Both TF and TFC showed broad peaks around 3274 and 3271 cm^{-1} resulting from vibrational stretching O-H bonds of hydroxyl (-OH) groups [45]. The peaks observed around 2918 and 2857 cm^{-1} of TF and 2919 and 2854 cm^{-1} of TFC could result from vibrational stretching of C-H bonds of -CH groups [45]. The peaks observed around 1600 cm^{-1} in both TF and TFC, resulted from vibrational stretching of C=C bonds [45]. The peaks observed around 1017 and 1018 cm^{-1} in FTIR spectra of TF and TFC, respectively, could have resulted from vibrational stretching of C-N bonds [3,45].

Figure 3 (a and b) represents FESEM images of TFC at different magnifications showing layered morphology with voids in between, which could promote access for electrolyte ions into deeper regions of TFC, thereby improving EDL formation [51].

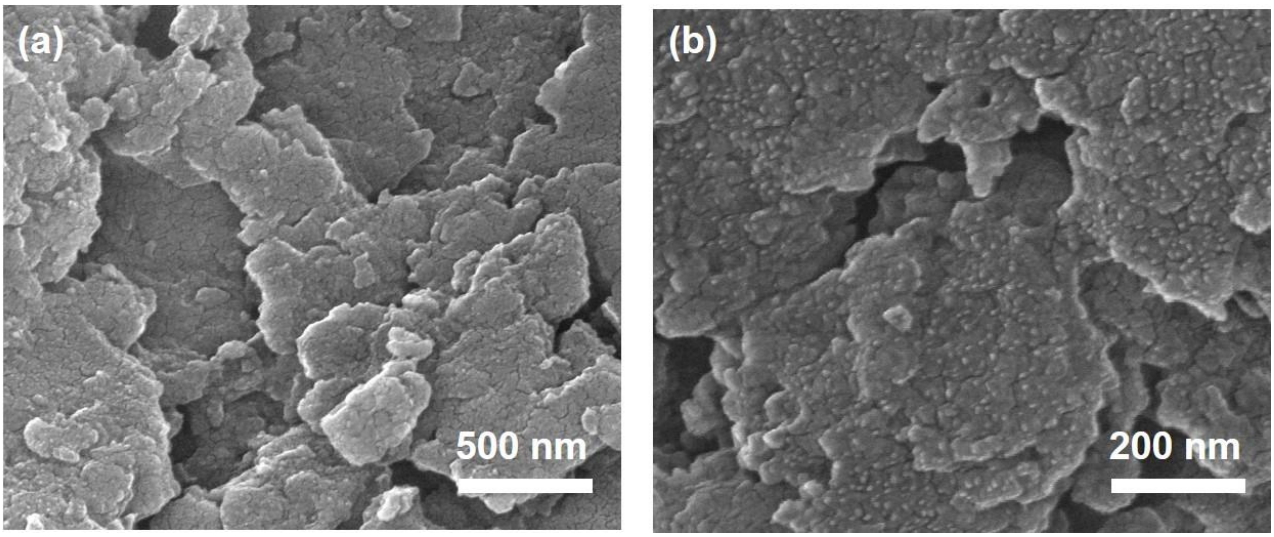

Figure 3. *(a) and (b) FESEM images depicting surface morphology of TFC*

Figure 4 (a) illustrates the TGA curve of TFC in which a weight loss of around 6 % was observed when heated up to 100 °C, which could be associated with water [52]. TFC lost 65 % of its weight when heated from 100 to 800 °C, which could be assigned to the degradation of lignin structures and removal of volatiles [53]. Figure 4 (b) illustrates the water contact angle of TFC with a contact angle of 52°, determining its hydrophilic property, which could improve the formation of EDL [54]. This hydrophilic nature of TFC could be attributed to the presence of -OH groups, as confirmed from FTIR data [45].

Figure 5(a) depicts the N_2 adsorption-desorption isotherm of TFC and the Brunauer–Emmett–Teller (BET) surface area of TFC was calculated to be around 17 $m^2 g^{-1}$. Figure 5(b) represents pore size distribution in TFC, where dV_o and D represent differential pore volume and pore diameter, respectively, while the average pore diameter was found to be around 2.8 nm.

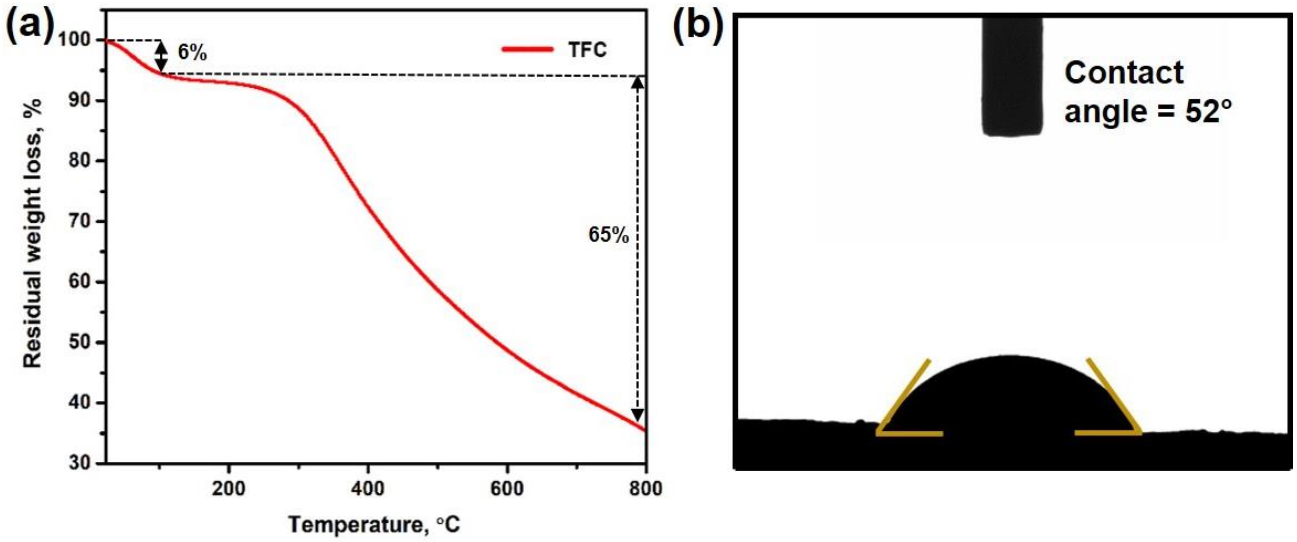

Figure 4. *(a) TGA curve and (b) contact angle measurement of TFC*

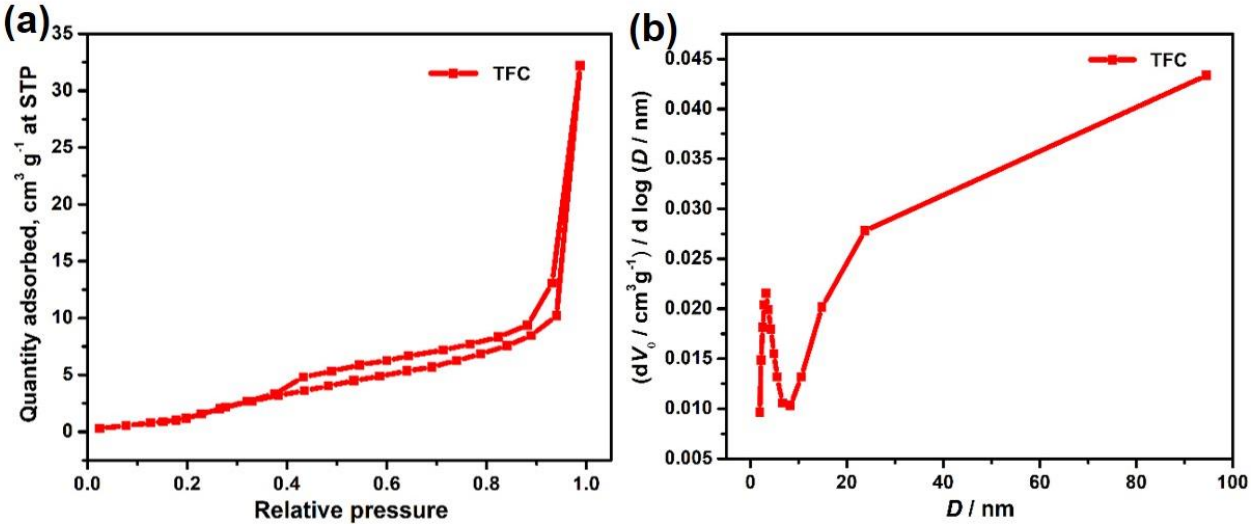

Figure 5. *(a) N_2 adsorption-desorption isotherm and (b) pore size distribution in TFC*

Electrochemical characterizations

Full cell studies

The supercapacitive behaviour of the fabricated TFC-based full-cell was tested using techniques like CV, GCD and EIS. Figure 6(a) illustrates the CV curves of TFC at different scan rates confirming superior capacitive behaviour with good reversibility and rate probability [55]. Figure 6 (b)

represents GCD curves of TFC at diverse constant current densities. The specific capacitance (C_s), specific energy (E_s) and specific power (P_s) of TFC-based symmetric SC were calculated using equations (1-3) [56]:

$$C_S = 2\frac{I\Delta t}{m\Delta V} \quad (1)$$

$$E_S = \frac{C_S \Delta V^2}{8} \quad (2)$$

$$P_S = \frac{E_S}{\Delta t} \quad (3)$$

where I, ΔV, Δt and m represent constant discharge current, discharge voltage, discharge time and mass of TFC (0.8 mg) on each electrode, respectively. Figure 6 (c) illustrates the Ragone plot of TFC. At 0.2 A g^{-1} constant current density, TFC exhibited exceptional C_s of 118.4 F g^{-1}. At a P_s of 0.1 kW kg^{-1}, TFC exhibited an E_s of 4.1 Wh kg^{-1}. Table 1 represents the experimental data obtained from GCD studies of TFC, while Table 2 illustrates the comparison of TFC's supercapacitive performance with carbon-based materials derived from some other flowers.

Table 1. *Experimental data obtained from GCD of TFC in full-cell studies*

Current density, A g^{-1}	IR drop, V	Discharge time, s	Specific capacitance, F g^{-1}
0.2	0.028	148	118.4
0.5	0.062	55	110
1	0.108	26	104
2	0.195	12	96
5	0.56	4.5	90

Table 2. *Comparison of TFC supercapacitive performance with carbon-based materials derived from flowers*

Precursor	Activating agent	Measurement	Specific capacitance, F g^{-1}	Reference
Cherry blossom petals	—	2-electrode	154 at 10 mV s^{-1}	[37]
Rose flower	KOH	3-electrode	208 at 0.5 A g^{-1}	[38]
Willow catkin	—	3-electrode	251 at 0.5 A g^{-1}	[39]
Willow catkin	KOH	3-electrode	292 at 1 A g^{-1}	[40]
Willow catkin	KOH	3-electrode	298 at 0.5 A g^{-1}	[41]
Willow catkin	KOH	3-electrode	340 at 0.1 A g^{-1}	[42]
Palmyra palm flowers	KOH	3-electrode	155 at 1 A g^{-1}	[57]
TF	NaOH	3-electrode	200 at 2 A g^{-1}	[45]
TF	—	2-electrode	118.4 at 0.2 A g^{-1}	This work

The cyclic stability of TFC was investigated by performing 6000 GCD cycles at a constant current density of 2 A g^{-1}. Figure 7 (a and b) represents the CV and GCD curves of TFC before and after cycling for 6000 cycles. Figure 7 (c) illustrates the cyclic stability of TFC for 6000 GCD cycles, where TFC retained 92 % of its initial capacitance. EIS studies were conducted at 0 V, using an alternating signal of 5 mV amplitude and the frequency range from 100 kHz to 0.1 Hz. Figure 7 (d) illustrates Nyquist plots of TFC before and after cycling for 6000 GCD cycles, which indicates a slight increase in cell impedance after cycling.

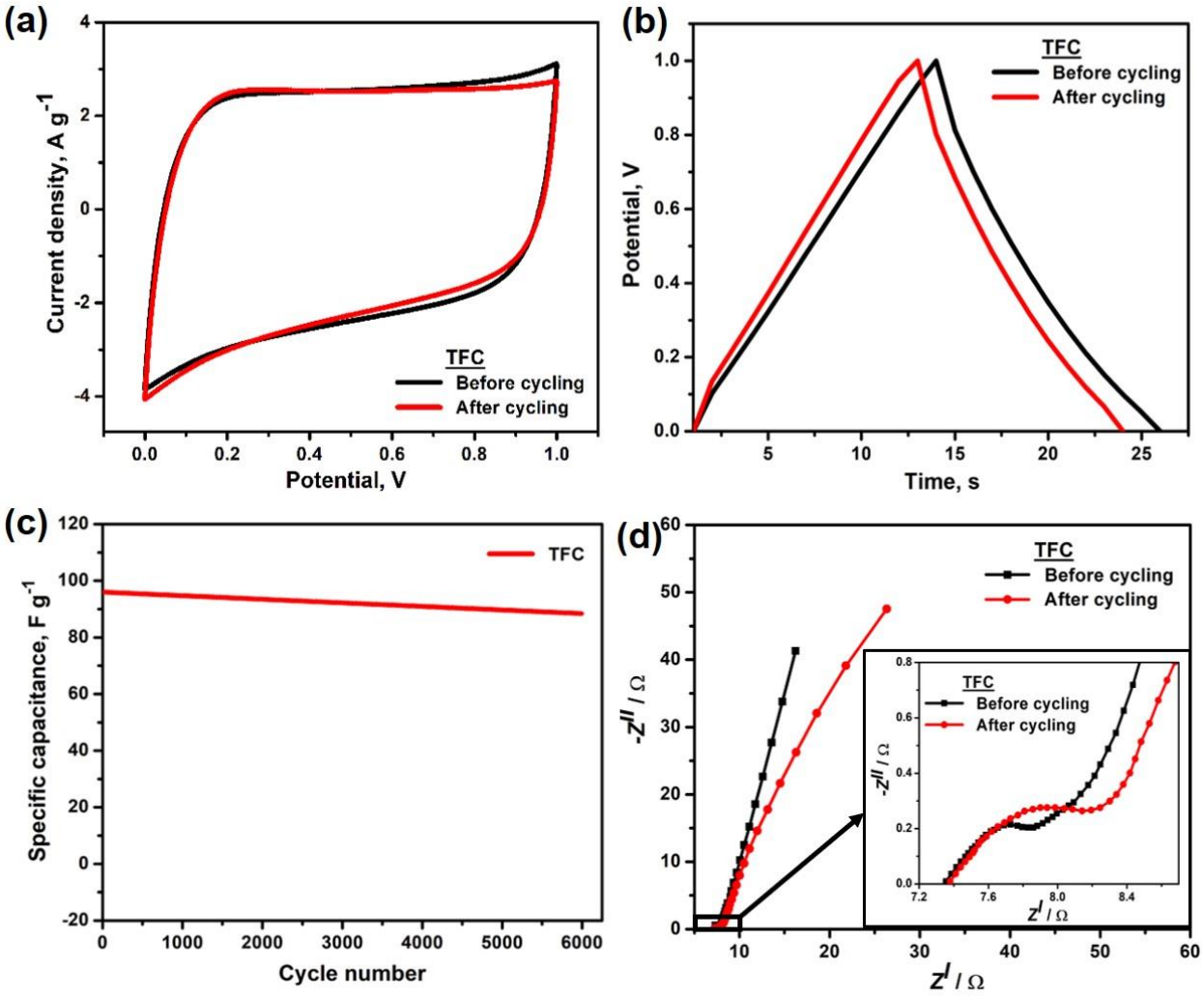

Figure 7. *(a) CV curves of TFC at 50 mV s^{-1} and (b) GCD curves of TFC at 1 A g^{-1}, before and after cycling; (c) cyclic stability of TFC for 6000 GCD cycles at 2 A g^{-1}; (d) Nyquist plots of TFC before and after cycling; inset image shows the magnified image of the high frequency region of Nyquist plots*

Conclusions

TF waste was used as a precursor to obtain TFC, a flower waste-derived carbon-based material through thermal decomposition and its physico-chemical properties were investigated. The practicality and applicability of TFC as potential electrode material in EDLCs was determined by evaluating supercapacitive behaviour of fabricated TFC-based SC using techniques like CV, GCD and EIS. At 0.2 A g^{-1} constant current density, TFC exhibited an exceptional specific capacitance of 118.4 F g^{-1}. At a P_s of 0.1 kW kg^{-1}, TFC exhibited an E_s of 4.1 Wh kg^{-1}. TFC showed superior cyclic stability by preserving 92 % of its original capacitance in spite of 6000 GCD cycles. The layered morphology of TFC and presence of voids, as confirmed from FESEM analysis, promote efficient access of electrolyte ions into deeper regions of TFC, thereby enhancing EDL formation. Water contact angle measurements of TFC confirmed its hydrophilic nature, which could be attributed to the presence of -OH groups in TFC as confirmed from FTIR analysis. This hydrophilic nature of TFC could have contributed to the superior supercapacitive behaviour of TFC, establishing it as a potential flower-waste derived carbon-based electrode material for SCs.

Acknowledgements: *The authors are grateful to Er. Koneru Satyanarayana Garu, Hon'ble President, Koneru Lakshmaiah Education Foundation (Deemed to be University) for providing infrastructure to carry out this work. The authors thank Prof. Y. Anjaneyulu, Director, CAES, KLEF and*

Dr. K. Naga Mahesh, Nanosol Energy Pvt Ltd, Hyderabad for their support. The authors thank the MARC, BIT, Bengaluru for surface area and porosity measurement, the DST and the SAIF, IIT Madras, Chennai for FESEM observation, the CRF, CeNS, Bengaluru for contact angle measurement and the CoExAMMPC, VFSTR, Guntur, A. P. for XRD, TGA and FTIR measurements.

References

[1] P. Dixit, S. Tripathi, K. N. Verma, *International Research Journal of Pharmacy* **4(1)** (2013) 43-48. https://irjponline.com/admin/php/uploads/1566_pdf.pdf

[2] S. Doda, O. Sahu, *Materials Today: Proceedings* **48** (2022) 932-937. https://doi.org/10.1016/j.matpr.2021.05.309

[3] M. S. Waghmode, A. B. Gunjal, N. N. Nawani, N. N. Patil, *Waste and Biomass Valorization* **9(1)** (2018) 33-43. https://doi.org/10.1007/s12649-016-9763-2

[4] P. Singh, U. Bajpai, *Environmental Progress & Sustainable Energy* **31(4)** (2012) 637-641. https://doi.org/10.1002/ep. 10589

[5] A. Mahindrakar, *Indian Journal of Pure and Applied Biosciences* **6(2)** (2018) 325-329. http://dx.doi.org/10.18782/2320-7051.5357

[6] M. Makhania, A. Upadhyay, *International Journal of Innovative and Emerging Research in Engineering* **2(2)** (2015) 145-147. http://ijiere.com/Finalpaper/Finalpaper20153110294170_deleted.pdf

[7] V. Kumar, S. Kumari, P. Kumar**,** in: *Environmental degradation: causes and remediation strategies* **1** (2020) 154. https://doi.org/10.26832/aesa-2020-edcrs-011

[8] S. Herou, P. Schlee, A.B. Jorge, M. Titirici, *Current Opinion in Green and Sustainable Chemistry* **9** (2018) 18-24. https://doi.org/10.1016/j.cogsc.2017.10.005

[9] A. Afif, S. M. Rahman, A. T. Azad, J. Zaini, M. A. Islan, A. K. Azad, *Journal of Energy Storage* **25** (2019) 100852. https://doi.org/10.1016/j.est.2019.100852

[10] X. Chen, R. Paul, L. Dai, *National Science Review* **4(3)** (2017) 453-489. https://doi.org/10.1093/nsr/nwx009

[11] V. N. K. S. K. Nersu, B. R. Annepu, S. S. B. Patcha, S. S. Rajaputra, *Journal of Electrochemical Science and Engineering* **12(3)** (2022) 451-462. https://doi.org/10.5599/jese.1310

[12] Y. Gong, D. Li, C. Luo, Q. Fu, C. Pan, *Green Chemistry* **19(17)** (2017) 4132-4140. https://doi.org/10.1039/C7GC01681F

[13] Y. Wang, Z. Zhao, W. Song, Z. Wang, X. Wu, *Journal of Materials Science* **54(6)** (2019) 4917-4927. https://doi.org/10.1007/s10853-018-03215-8

[14] Y. Zhang, S. Liu, X. Zheng, X. Wang, Y. Xu, H. Tang, J. Luo, *Advanced Functional Materials* **27(3)** (2017) 1604687. https://doi.org/10.1002/adfm.201604687

[15] S.Y. Lu, M. Jin, Y. Zhang, Y.B. Niu, J.C. Gao, C. M. Li, *Advanced Energy Materials* **8(11)** (2018) 1702545. https://doi.org/10.1002/aenm.201702545

[16] W. Liu, J. Mei, G. Liu, Q. Kou, T. Yi, S. Xiao, *ACS Sustainable Chemistry Engineering* **6(9)** (2018) 11595-11605. https://doi.org/10.1021/acssuschemeng.8b01798

[17] C. Wang, D. Wu, H. Wang, Z. Gao, F. Xu, K. Jiang, *Journal of Materials Chemistry A* **6(3)** (2018) 1244-1254. https://doi.org/10.1039/C7TA07579K

[18] X. Tian, H. Ma, Z. Li, S. Yan, L. Ma, F. Yu, C. Wong, *Journal of Power Sources* **359** (2017) 88-96. https://doi.org/10.1016/j.jpowsour.2017.05.054

[19] H. Feng, H. Hu, H. Dong, Y. Xiao, Y. Cai, B. Lei, M. Zheng, *Journal of Power Sources* **302** (2016) 164-173. https://doi.org/10.1016/j.jpowsour.2015.10.063

[20] I. I. Misnon, N. K. M. Zain, R. Abd Aziz, B. Vidyadharan R. Jose, *Electrochimica Acta* **174** (2015) 78-86. https://doi.org/10.1016/j.electacta.2015.05.163

[21] U. Thubsuang, S. Laebang, N. Manmuanpom, S. Wongkasemjit, T. Chaisuwan, *Journal of Materials Science* **52(11)** (2017) 6837-6855. https://doi.org/10.1007/s10853-017-0922-z

[22] H. Wang, Z. Xu, A. Kohandehghan, Z. Li, K. Cui, X. Tan, D. Mitlin, *ACS Nano* **7(6)** (2013) 5131-5141. https://doi.org/10.1021/nn400731g
[23] L. Ji, B. Wang, Y. Yu, N. Wang, J. Zhao, *Electrochimica Acta* **331** (2020) 135348. https://doi.org/10.1016/j.electacta.2019.135348
[24] C. Zequine, C.K. Ranaweera, Z. Wang, P. R. Dvornic, P. K. Kahol, S. Singh, R. K. Gupta, *Scientific Reports* **7(1)** (2017) 1174. https://doi.org/10.1038/s41598-017-01319-w
[25] S. Qu, J. Wan, C. Dai, T. Jin, F. Ma, *Journal of Alloys and Compounds* **751** (2018) 107-116. https://doi.org/10.1016/j.jallcom.2018.04.123
[26] A. K. Mondal, K. Kretschmer, Y. Zhao, H. Liu, C. Wang, B. Sun, G. Wang, *Chemistry-A European Journal* **23(15)** (2017) 3683-3690. https://doi.org/10.1002/chem.201605019
[27] S. T. Senthilkumar, R. K. Selvan, *Chem Electro Chem* **2(8)** (2015) 1111-1116. https://doi.org/10.1002/celc.201500090
[28] G. Zhu, L. Ma, H. Lv, Y. Hu, T. Chen, R. Chen, J. Liu, *Nanoscale* **9(3)** (2017) 1237-1243. https://doi.org/10.1039/C6NR08139H
[29] J. Xia, N. Zhang, S. Chong, Y. Chen, C. Sun, *Green Chemistry* **20(3)** (2018) 694-700. https://doi.org/10.1039/C7GC03426A
[30] M. Chen, X. Kang, T. Wumaier, J. Dou, B. Gao, Y. Han, L. Zhang, *Journal of Solid State Electrochemistry* **17(4)** (2013) 1005-1012. https://doi.org/10.1007/s10008-012-1946-6
[31] X. Yan, Y. Jia, L. Zhuang, L. Zhang, K. Wang, X. Yao, *ChemElectroChem* **5(14)** (2018) 1874-1879. https://doi.org/10.1002/celc.201800068
[32] M. Liu, J. Niu, Z. Zhang, M. Dou, F. Wang, *Nano Energy* **51** (2018) 366-372. https://doi.org/10.1016/j.nanoen.2018.06.037
[33] W. Qian, F. Sun, Y. Xu, L. Qiu, C. Liu, S. Wang, F. Yan, *Energy and Environmental Science* **7(1)** (2014) 379-386. https://doi.org/10.1039/C3EE43111H
[34] F. Gao, J. Qu, C. Geng, G. Shao, M. Wu, *Journal of Materials Chemistry A* **4(19)** (2016) 7445-7452. https://doi.org/10.1039/C6TA01314G
[35] Z. Li, L. Zhang, B.S. Amirkhiz, X. Tan, Z. Xu, H. Wang, D. Mitlin, *Advanced Energy Materials* **2(4)** (2012) 431-437. https://doi.org/10.1002/aenm.201100548
[36] Q. Wang, Q. Cao, X. Wang, B. Jing, H. Kuang, L. Zhou, *Journal of Power Sources* **225** (2013) 101-107. https://doi.org/10.1016/j.jpowsour.2012.10.022
[37] X. Yu, Y. Wang, L. Li, H. Li, Y. Shang, *Scientific Reports* **7(1)** (2017) 45378. https://doi.org/10.1038/srep45378
[38] C. Zhao, Y. Huang, C. Zhao, X. Shao, Z. Zhu, *Electrochimica Acta* **291** (2018) 287-296. https://doi.org/10.1016/j.electacta.2018.09.136
[39] S. Gao, X. Li, L. Li, X. Wei, *Nano Energy* **33** (2017) 334-342. https://doi.org/10.1016/j.nanoen.2017.01.045
[40] L. Xie, G. Sun, F. Su, X. Guo, Q. Kong, X. Li, C. M. Chen, *Journal of Materials Chemistry A* **4(5)** (2016) 1637-1646. https://doi.org/10.1039/C5TA09043A
[41] Y. Li, G. Wang, T. Wei, Z. Fan, P. Yan, *Nano Energy* **19** (2016) 165-175. https://doi.org/10.1016/j.nanoen.2015.10.038
[42] K. Wang, N. Zhao, S. Lei, R. Yan, X. Tian, J. Wang, Y. Song, D. Xu, Q. Guo, L. Liu, *Electrochimica Acta* **166** (2015) 1-11. https://doi.org/10.1016/j.electacta.2015.03.048
[43] B. Salehi, M. Valussi, M. F. B. Morais-Braga, J. N. P. Carneiro, A. L. A. B. Leal, H. D. M. Coutinho, J. *Molecules* **23(11)** (2018) 2847. https://doi.org/10.3390/molecules23112847
[44] V. Kumar, R. S. Singh, M. Pal, M. D. Ojha, R. B. Verma, R. K. Verma, A. P. Singh, *Journal of Pharmacognosy and Phytochemistry* **8(1)** (2019) 819-822. https://www.phytojournal.com/archives/2019/vol8issue1/PartN/8-1-158-748.pdf

[45] G. K. Gupta, P. Sagar, M. Srivastava, A. K. Singh, J. Singh, S. K. Srivastava, A. Srivastava, *International Journal of Hydrogen Energy* **46(77)** (2021) 38416-38424. https://doi.org/10.1016/j.ijhydene.2021.09.094
[46] S. S. Rajaputra, N. Pennada, A. Yerramilli, N. M. Kummara, *Journal of Electrochemical Energy Conversion and Storage* **18(4)** (2021) 041008. https://doi.org/10.1115/1.4051143
[47] S. S. Rajaputra, N. Pennada, A. Yerramilli, N. M. Kummara, *Ionics* **27(9)** (2021) 4069-4082. https://doi.org/10.1007/s11581-021-04144-4
[48] S. S. Rajaputra, N. Pennada, A. Yerramilli, N. M. Kummara, *Journal of Electrochemical Science and Engineering* **11(3)** (2021) 197-207. https://doi.org/10.5599/jese.1031
[49] S. López-Romero, J. Chávez-Ramírez, *Matéria (Rio de Janeiro)* **12** (2007) 487-493. https://doi.org/10.1590/S1517-70762007000300009
[50] S. Lanfredi, M.A. Nobre, P.S. Poon, J. Matos, *Molecules* **25(1)** (2020) 96. https://doi.org/10.3390/molecules25010096
[51] T. Eguchi, D. Tashima, M. Fukuma, S. Kumagai, *Journal of Cleaner Production* **259** (2020) 120822. https://doi.org/10.1016/j.jclepro.2020.120822
[52] P. Singh, R. Singh, A. Borthakur, S. Madhav, V. K. Singh, D. Tiwary, P. K. Mishra, *Waste Management* **77** (2018) 78-86. https://doi.org/10.1016/j.wasman.2018.04.041
[53] R. Singh, J.N. Babu, R. Kumar, P. Srivastava, P. Singh, A.S. Raghubanshi, *Ecological Engineering* **77** (2015) 324-347. https://doi.org/10.1016/j.ecoleng.2015.01.011
[54] H. Yang, Z. Bo, J. Yan, K. Cen, *International Journal of Heat and Mass Transfer* **133** (2019) 416-425. https://doi.org/10.1016/j.ijheatmasstransfer.2018.12.134
[55] D. P. Dubal, N. R. Chodankar, D.-H. Kim, P. R. Gomez, *Chemical Society Reviews* **47** (2018) 2065-2129. https://doi.org/10.1039/C7CS00505A
[56] H. Wang, H. Yi, X. Chen, X. Wang, *Journal of Materials Chemistry A* **2(9)** (2014) 3223-3230. https://doi.org/10.1039/C3TA15046A
[57] S. J. Rajasekaran, V. Raghavan, *Journal of Electrochemical Science and Engineering* **12(3)** (2022) 545-556. https://doi.org/10.5599/jese.1314